Substrate adaptability of β-lactamase

Sun, J.

Chapter 3

A low-barrier proton shared between two aspartates acts as a conformational switch that changes the substrate specificity of the β-lactamase BlaC

Abstract

Serine β-lactamases inactivate β-lactam antibiotics in a two-step mechanism comprising acylation and deacylation. For the deacylation step, a water molecule is activated by a conserved glutamate residue to release the adduct from the enzyme. The third-generation cephalosporin ceftazidime is a poor substrate for the class A β-lactamase BlaC from *Mycobacterium tuberculosis* but it can be hydrolyzed faster when the active site pocket is enlarged, as was reported for mutant BlaC P167S. However, the conformational change displaces the conserved glutamate (Glu166), suggesting it is not required for deacylation of the ceftazidime adduct. Here, we report the characterization of wild type BlaC and BlaC E166A at various pH values. The presence of Glu166 strongly enhances activity against nitrocefin but not ceftazidime, indicating it is indeed not required for deacylation of the adduct of the latter substrate. At high pH wild type BlaC was found to exist in two states, one of which converts ceftazidime much faster, resembling the open state previously reported for the BlaC mutant P167S. The pH-dependent switch between the closed and open states is caused by the loss of a low-barrier hydrogen bond, a proton shared between Asp172 and Asp179 at high pH. These results illustrate how readily shifts in substrate specificity can occur as a consequence of subtle changes in protein structure.

Introduction

The activity and substrate specificity of enzymes is related to their conformational freedom, which is illustrated by phenomena such as allostery,[169,170] order-disorder transition,[171,172] substrate-induced conformational change,[173,174] and loop and domain movements.[175] β-Lactamases are responsible for the hydrolysis of β-lactam antibiotics and these enzymes have evolved new substrate specificities under changing selection pressures due to the application of successive generations of antibiotics. The gain of function of activities for new substrates is often accompanied by the loss of activity for the original substrates.[95,110,137] A case in point is the increased hydrolysis of oxyimino cephalosporins such as ceftazidime at the expense of the conversion of penicillin-like substrates. The Ω-loop, a structurally important region in class A β-lactamases that lines the active site, plays a crucial role in modulating the enzyme activity and substrate specificity.[176-178] Its conformation influences the relative activity of the enzyme towards different substrates. In the triple mutant 165-YYG-167 of TEM-1 β-lactamase, the Ω-loop has been reported to be in an open conformation and the enzyme showed an altered substrate profile, with increased activity for ceftazidime and decreased activity for all other β-lactams.[110,133] Bowman and co-workers discovered that TEM-1 features a cryptic pocket, which increases the hydrolysis of benzylpenicillin in the open form, and favors the hydrolysis of cefotaxime when closed.[95] A cryptic pocket was also found in CTX-M β-lactamase. In this case, ligand binding pushed the Ω-loop open and ceftazidime activity increased.[135,136] In a recent study, our group reported that the P167S (Ambler numbering[73]) variant of β-lactamase BlaC encoded on the *Mycobacterium tuberculosis* (Mtb) chromosome, exists in two states in the absence of substrate. Crystallography revealed the structures of the two states, one being in a (semi-)closed state, resembling the WT structure and the other having the Ω-loop wide open, creating a large active site pocket. The open state showed increased hydrolysis of ceftazidime.[179] Interestingly, in the structure of the open state, Glu166 was pointing into the solvent, away from the active site. This residue is highly conserved and considered to be the general base in the deacylation phase of the hydrolysis reaction.[141,180] Mutagenesis studies have illuminated its critical role in the hydrolysis

of β-lactam antibiotics. Shortening (E166D) or lengthening (S-carboxymethylcysteine mutant) the side-chain of E166 in β-lactamase I of *Bacillus cereus* resulted in strongly decreased activity on penicillin substrates[181,182] or 2nd generation cephalosporins.[183] The mutant E166A is almost totally incapable of deacylation and has been used to generate stable acyl-enzyme intermediates.[182-186] However, the E166A mutant of β-lactamase I retained some activity for nitrocefin hydrolysis, suggesting that other groups in the active site could take over the role as general base to activate the catalytic water molecule during deacylation.[182] Active site residue Lys73 has been proposed as a candidate.[155] In the triple mutant of TEM-1 mentioned above, the presence of Tyr166, which is still located in a position similar to that of Glu166, resulted in a shift of the optimal pH for hydrolysis, suggesting that Tyr acts as the general base in this variant.[133] In the structure of BlaC P167S in the open state, Glu166 was much too far from the active site to be functional, which may indicate that ceftazidime hydrolysis does not require this residue.

To investigate whether Glu166 has a role in ceftazidime hydrolysis, we compared BlaC E166A with WT enzyme at various pH values through a combination of kinetic experiments, NMR spectroscopy and protein crystallography. The results show that Glu166 is important for nitrocefin hydrolysis but activity against ceftazidime is similar for BlaC WT and E166A at neutral and high pH and even better for the mutant at pH 5, indicating that Glu166 is not required for activity. Surprisingly, we also found that WT BlaC occurs in two states at high pH. The high pH form resembles the state of BlaC P167S with the Ω-loop opened up. We show that the conformational shift in the Ω-loop at high pH is caused by deprotonation of the Asp172/Asp179 pair of residues, which share a low-barrier H-bond. This study illustrates how readily substrate specificity can be altered by subtle changes in the protein structure.

Results

BlaC WT shows biphasic kinetics at high pH.

Escherichia coli cells producing BlaC E166A were more resistant against ceftazidime and ceftriaxone than cells producing BlaC WT (Figure S3.1). To characterize the enzymes *in vitro*, BlaC WT and E166A were overproduced and purified and the

kinetic parameters of hydrolysis of nitrocefin, ceftazidime, and cefepime were determined at pH 5.0, 6.5 and 8.0 (Table 3.1). BlaC E166A displays reduced efficiency for hydrolysis of nitrocefin, exhibiting a reduction in the specificity constant (k_{cat}/K_M^{app}) compared to that of BlaC WT, which varies with pH (11-fold, 100-fold and 7-fold at pH 5, 6.5 and 8, respectively). The optimal pH for BlaC WT hydrolysis of nitrocefin is 6.5, in line with previously reported values,[144,187] whereas for BlaC E166A, it is minimal at this pH. These results indicate a role for Glu166 in nitrocefin hydrolysis.

Ceftazidime is a poor substrate for BlaC with catalytic efficiencies that are two orders of magnitude lower than for nitrocefin.[72] Hydrolysis by BlaC WT shows biphasic kinetics at pH 8 and 9, with an initial burst followed by a linear second phase (Figure 1a). The amplitude of the burst phase is dependent on the substrate concentration and greatly exceeds the enzyme concentration for high concentrations of ceftazidime, indicating the first phase of the curve is not caused by accumulation of an enzyme intermediate in the first round of catalysis but is due to branched kinetics (Figure S3.2a). At lower pH, an initial phase with a very small amplitude may be present but is barely detectable. In contrast, the E166A mutant exhibits clear biphasic behavior under all pH conditions (Figure 3.1a). The highest initial rate of the first phase is found at pH 5, followed by pH 6.5, 8, and 9. As the first phase is not observed for BlaC at pH 5 and 6.5, we consider the observed linear curve equivalent to the second phase observed at pH 8. The velocity of this phase is not strongly dependent on the pH for BlaC WT and E166A and the apparent K_M of this phase is low (Table 3.1).

These results indicate that the removal of the functional group in the E166A mutant has no negative effect on ceftazidime hydrolysis, suggesting the Glu is not needed for catalysis. Furthermore, high pH favors the catalytic reaction for BlaC WT. Similar results were observed for cefepime hydrolysis, also exhibiting efficient catalysis at pH 8 for both BlaC WT and E166A (Table 3.1, Figure S3.3). Biphasic behavior for ceftazidime hydrolysis was observed before for BlaC P167S and was shown to be a consequence of branched pathway kinetics, indicative of a conformation change.[179] Branched pathways could arise either through the chemical rearrangement of the acyl moiety or by a conformational change of the enzyme,[108,145,179] suggesting that BlaC WT and E166A could exist in two conformations under certain conditions, like P167S.

Table 3.1 Kinetic parameters for ceftazidime, nitrocefin and cefepime hydrolysis by BlaC WT and mutants at 25 °C. The values and (propagated) errors present the averages and standard deviations over three experiments. For biphasic kinetics the parameters for both phases are given. Parameters for monophasic kinetics are listed under Phase 2.

			Phase 1			Phase 2		
Substrate	Enzyme	Parameters	pH 5	pH 6.5	pH 8	pH 5	pH 6.5	pH 8
Ceftazidime	WT	k_{cat} (s^{-1})			0.12 ± 0.03			0.0012 ± 0.0006
		K_M^{app} (μM)			94 ± 16			2.0 ± 0.4
		k_{cat}/K_M^{app} (10^3 $M^{-1}s^{-1}$)			1.3 ± 0.3	0.4 ± 0.2	0.2 ± 0.1	0.6 ± 0.3
	E166A	k_{cat} (s^{-1})	0.3 ± 0.1			0.0043 ± 0.0005	0.0011 ± 0.0004	0.0015 ± 0.0002
		K_M^{app} (μM)	220 ± 15			1.8 ± 0.5	2 ± 1	2.0 ± 0.3
		k_{cat}/K_M^{app} (10^3 $M^{-1}s^{-1}$)	1.5 ± 0.2	0.3 ± 0.1	2.4 ± 0.9	2 ± 1	0.6 ± 0.4	0.8 ± 0.3
	D179N	k_{cat} (s^{-1})				0.05 ± 0.01	0.05 ± 0.003	0.004 ± 0.002
		K_M^{app} (μM)				148 ± 10.1	148 ± 10.6	10 ± 4.4
		k_{cat}/K_M^{app} (10^3 $M^{-1}s^{-1}$)	0.8 ± 0.2	0.7 ± 0.2	0.5 ± 0.1	0.3 ± 0.1	0.3 ± 0.03	0.4 ± 0.02
	D172N	k_{cat} (s^{-1})				0.002 ± 0.001	0.003 ± 0.002	0.004 ± 0.001
		K_M^{app} (μM)				90 ± 26	150 ± 15	160 ± 31
		k_{cat}/K_M^{app} (10^3 $M^{-1}s^{-1}$)	0.4 ± 0.3	0.4 ± 0.1	0.5 ± 0.1	0.02 ± 0.01	0.02 ± 0.01	0.02 ± 0.01
Nitrocefin	WT	k_{cat} (s^{-1})				29 ± 6	120 ± 8	12 ± 1
		K_M^{app} (μM)				133 ± 43	215 ± 19	80 ± 22
		k_{cat}/K_M^{app} (10^5 $M^{-1}s^{-1}$)				2.2 ± 0.3	5.6 ± 0.6	2.0 ± 0.4
	E166A	k_{cat} (s^{-1})				5 ± 2	0.3 ± 0.1	0.13 ± 0.05
		K_M^{app} (μM)				215 ± 79	28 ± 14	4 ± 2
		k_{cat}/K_M^{app} (10^5 $M^{-1}s^{-1}$)				0.2 ± 0.1	0.05 ± 0.01	0.3 ± 0.1
Cefepime	WT	k_{cat} (s^{-1})						0.019 ± 0.001
		K_M^{app} (μM)						11 ± 6
		k_{cat}/K_M^{app} (10^3 $M^{-1}s^{-1}$)			0.8 ± 0.1	0.2 ± 0.1	0.11 ± 0.05	1.76 ± 0.01
	E166A	k_{cat} (s^{-1})			0.03 ± 0.01	0.0011 ± 0.0005	0.0003 ± 0.0001	0.0011 ± 0.0002
		K_M^{app} (μM)			18 ± 7	1.5 ± 0.4	1.2 ± 0.3	14 ± 1
		k_{cat}/K_M^{app} (10^3 $M^{-1}s^{-1}$)	0.3 ± 0.1	0.4 ± 0.1	1.8 ± 0.9	0.5 ± 0.3	0.3 ± 0.1	0.08 ± 0.02

To gain further insight into the pH effect on substrate specificity, the initial velocities for hydrolysis of nitrocefin, ampicillin, meropenem, cefoxitin, cefuroxime, and ceftriaxone by BlaC WT were also measured at pH values 5, 7, 8, 8.5 and 9 (Figure 1b). If two phases were present, the initial velocities of the first phase were used. The optimal pH for nitrocefin, ampicillin, and cefoxitin hydrolysis was 5, whereas it was pH 8 for cefuroxime, ceftazidime, ceftriaxone, and cefepime, which all contain bulky side chains at the C7 position. These findings indicate that pH modulates substrate specificity of BlaC.

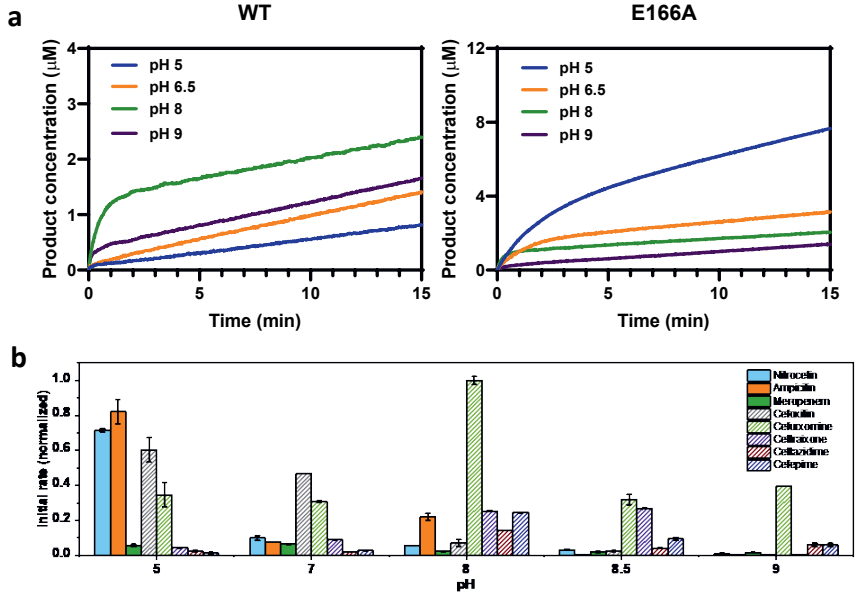

Figure 3.1 Substrate hydrolysis. **a)** Ceftazidime hydrolysis by BlaC WT (left) and E166A (right) at 25 ˚C and different pH values; **b)** Normalized initial rate of enzymatic reactions with different substrates at pH values between 5 to 9. The normalized initial rate is based on the highest observed initial rate of cefuroxime at pH 8, which was set to 1. Error bars represent the standard deviation from three experiments. Concentrations of substrate and BlaC were 25 μM and 1 μM, respectively, for all experiments shown in this figure.

BlaC changes conformation at high pH.

To assess whether BlaC WT and E166A could exist in different conformations at different pH, ^{1}H-^{15}N TROSY-HSQC spectra at pH values between 5 and 10 in 100 mM sodium phosphate buffer (NaPi) were obtained. At pH 8, for both BlaC WT and E166A, well-resolved double peaks were observed for multiple amides, indicating two conformations (Figures 3.2a and S3.4). With increasing pH, the peak intensities for one state (state B) increase, whereas those for the other state (state A) decrease. The two states reported before for BlaC P167S, an open and a (semi-)closed conformation, were observed at pH 6.5.[179] For this variant, single peaks are observed at pH 8, (Figure 3.2a). These results suggest that BlaC WT and E166A show a conformational change that resembles the one in BlaC P167S but with a shifted pK_a. By fitting the peak intensities, the pK_a values were determined to be 8.93 ± 0.04 for BlaC WT and 6.70 ± 0.03 for BlaC P167S (Figure 3.2b). Phosphate is known to bind to the carboxylate binding pocket in the active site,[149,152,179] affecting the populations of the two conformations in BlaC P167S.[179] To probe the effect of phosphate on the pK_a of BlaC WT, the pH titration was repeated in 100 mM MES (pH 5 and 6), HEPES (pH 7), and Tris buffers (pH 7.5, 8, 8.5, 9, and 10). In the absence of phosphate in the buffer, the pK_a for BlaC WT shifted by 0.83 units to 9.76 ± 0.02 and for BlaC P167S, a shift of 0.55 units was found, yielding a pK_a of 7.25 ± 0.01 (Figure 3.2b). In line with the lower pK_a for the transition to state B in the presence of phosphate, TROSY-HSQC spectra taken at phosphate concentrations ranging from 0 to 250 mM for BlaC WT (Figure 3.2c) show that the presence of phosphate causes a shift in the population of conformations towards state B. This finding is consistent with the behavior described for the P167S mutant.[179]

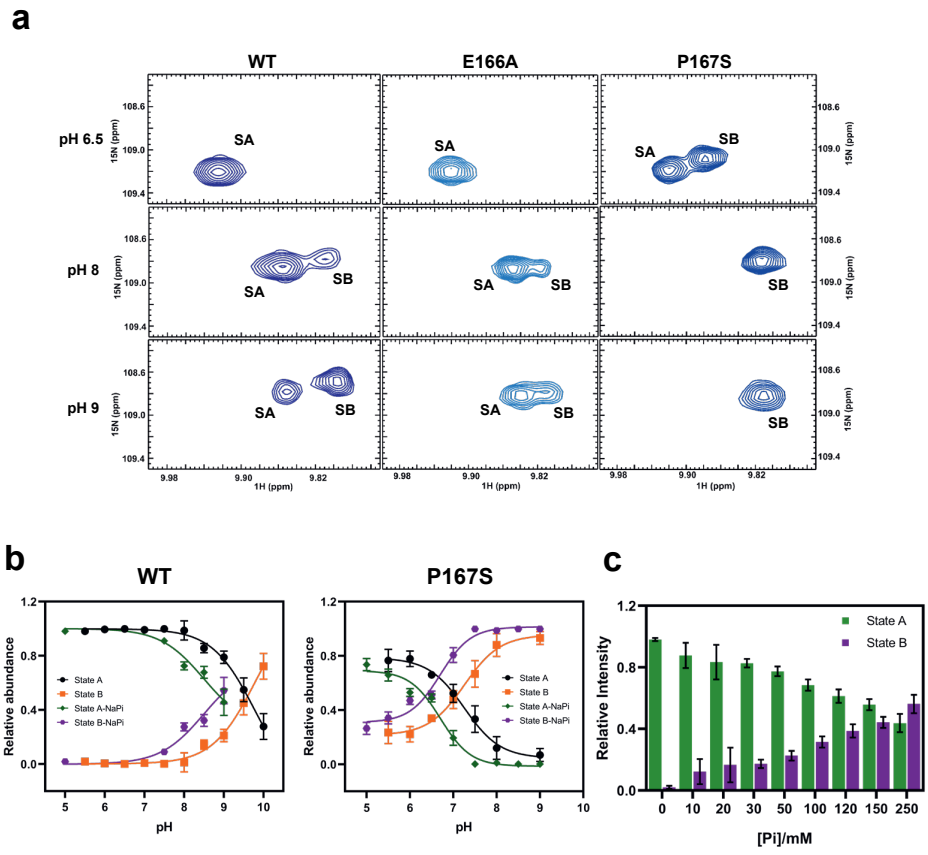

Figure 3.2 Two conformations of BlaC. **a)** Detail of TROSY-HSQC spectra of BlaC WT (navy), E166A mutant (sky-blue), and P167S mutant (blue) at pH 6.5, 8, and 9, showing the resonance of Gly120. SA and SB refer to state A and state B; **b)** The relative abundance of the two conformational states for BlaC WT and P167S mutant change in response to pH. The green and purple lines are in NaPi buffer, and the black and orange lines are in the buffer without NaPi. The relative abundance was averaged over 33 residues and the errors are the standard deviation over the data for these residues; **c)** Relative intensity of states A (green) and B (purple) of BlaC WT at pH 8 as a function of phosphate concentration. Intensities were averaged over 27 residues. The errors are the standard deviation over intensities of these residues.

The high pH structure of BlaC WT resembles the open state of P167S

Structure determination using crystallography was attempted at various pH conditions. The structures of BlaC WT at pH 5 (PDB ID: 5NJ2[149]) and pH 8 (PDB

ID: 2GDN[72]) have been reported and are very similar. We also obtained the crystal structure of BlaC WT at pH 8, but it shows a single conformation that it is identical to the ones previously published at pH 8 and 5. The crystallization process can lead to selective crystal formation of one of the conformations, so it may not be feasible to get the crystal structures of both states as was done for BlaC P167S.[179] Crystals of BlaC E166A were obtained at pH 5, pH 6.5, and pH 8. Due to the fragility of the crystal at pH 8, no structure could be determined. The structures of the crystals obtained at pH 5 and pH 6.5 were solved at 1.4 Å and 2.3 Å resolution, respectively (Table S3.1). They do not reveal significant structural differences and resemble the structure of BlaC WT (C_α RMSD 0.29 Å). The largest difference is that the loss of the hydrogen bond between Glu166 and Asn170 leads to a small displacement of the backbone of Asn170 that extends into the Ω-loop (Figure 3.3a). The peptide bond between Pro174 and Gly175 is flipped in E166A at pH 4.5 compared to the BlaC WT at pH 5. The averaged chemical shift perturbations (CSP) of amides of BlaC E166A at pH 5 and 6.5 compared to BlaC WT mapped on the structure of BlaC indicate that the mutation causes effects in a large part of the active site and the Ω-loop. The maps look similar for pH 5 and 6.5 (Figure 3.3b). These differences may underly the enhanced activity of BlaC E166A against ceftazidime compared to BlaC WT (Table 3.1) but do not explain why hydrolysis is much faster at pH 5 than at pH 6.5 (Figure 3.1a).

To characterize the two states of BlaC WT observed in solution at pH 8, the ^{1}H-^{15}N resonances were assigned by comparison to BlaC WT assignments at pH 6.5 and confirmed using an HNCA spectrum, obtained with a ^{13}C-^{15}N uniformly labelled sample. Of all amides, the resonances for 223 residues could be assigned. The split peaks relating to the two states have a minimum distance of ~12 Hz, indicating that the exchange rate between the states is in the slow regime ($\boldsymbol{k_{ex}} \ll 53\ s^{-1}$). The spectra of BlaC WT at pH 8.0 in NaPi were compared to those of BlaC P167S. For the residues of WT BlaC showing double peaks, the peaks of state B were found in similar positions as those observed in the P167S mutant at pH 8, suggesting that this conformation resembles the open form (Figure 3.4a and 3.4b). The chemical shift differences between the pairs of peaks of the two states of BlaC WT at pH 8 and those of BlaC P167S at pH 6.5 are very similar (Figure 3.4c). Therefore, it is concluded

that the two conformations in WT BlaC at pH 8 resemble the (semi)closed and open forms observed in the P167S mutant.

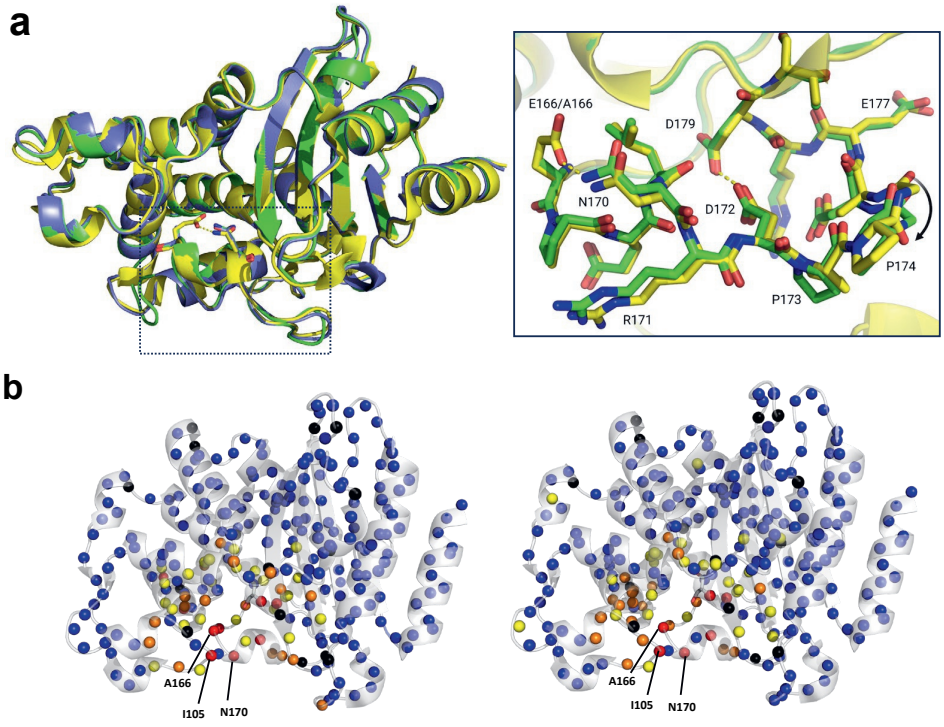

Figure 3.3 Structural effect of the Glu166 mutation. **a)** Crystal structure of BlaC E166A at pH 4.5 (green) and pH 6.5 (blue) overlaid with wild type structure at pH 5 (PDB entry 5NJ2[149], yellow). On the right, the Ω-loop is shown, representing the boxed area in the left picture. The Ω-loop is shown in sticks. The black arrow indicates the flipped peptide bond and the yellow dotted lines mark the potential H-bonds of Glu166/Asn170 and Asp172/Asp179; **b)** Average CSPs of BlaC E166A at pH 5 (left) and pH 6.5 (right), plotted on the crystal structure of BlaC WT (PDB entry 2GDN[72]) . Backbone amides are indicated as spheres. Yellow: $0.05 < CSP \leqslant 0.1$ ppm, orange: $0.1 < CSP \leqslant 0.15$ ppm, red: $CSP > 0.15$ ppm, blue: $CSP \leqslant 0.05$ ppm. Black: no data available (proline or unassigned)

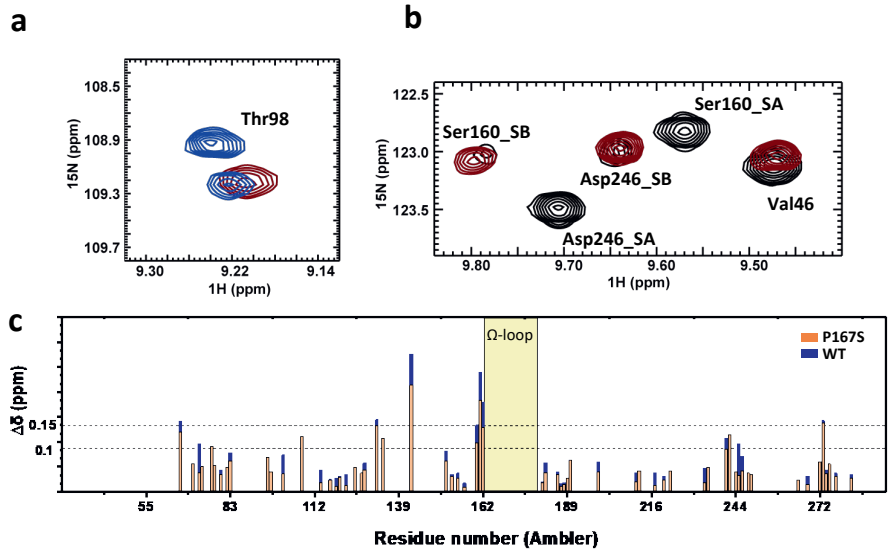

Figure 3.4 WT BlaC conformations resemble those of BlaC P167S. **a)** Details of TROSY-HSQC spectra of BlaC P167S at pH 6.5 (blue) and pH 8 (maroon) showing the resonances of Thr98; **b)** Details of TROSY-HSQC spectra of BlaC WT (black) and P167S (maroon) at pH 8.0. SA and SB refer to states A and B, respectively; **c)** Comparison of average chemical shift (eq. 3.3) differences for the backbone amides with double peaks of BlaC WT at pH 8.0 (blue) and P167S at pH 6.5 (orange) at 25°C in 100 mM NaPi. The dotted lines represent the CSP at 0.15 and 0.10 ppm.

The Asp172-Asp179 pair in the Ω-loop acts as the pH switch

The P167S mutation disrupts the stability of the Ω-loop by inducing a trans-conformation of the Glu166-Ser167 peptide bond.[179] Also mutations in Asp179 affect the stability of the Ω-loop of BlaC.[188] Therefore, we wondered whether the low-barrier H-bond (LBHB) between Asp172 and Asp179 was the titratable group in BlaC WT that causes the change in conformation. LBHBs[189,190] have been proposed to play a crucial role in catalytic reactions and protein flexibility.[191] The interatomic distance between the two heteroatoms of LBHBs is smaller than for regular H-bonds ($\leqslant$2.55 Å for O–O pairs; $\leqslant$2.65 Å for O–N pairs).[191,192] The H-bond between the carboxy groups of Asp172 and Asp179 is 2.5 Å and matches that of an LBHB (Figure 3.5a),

whereas in the structures of BlaC D172N and D179N (PDB ID:7A5W[158] and 8BTU[188]), the length of the H-bond between the Asp and Asn side chains increases to that of a regular H-bond, 2.7 Å and 2.8 Å, respectively (Figure 3.5b, 3.5d). The LBHB between two carboxy groups is expected to become deprotonated at a certain pH value, leading to repulsion between the two negatively charged carboxy groups. For an Asp-Asn H-bond deprotonation is not expected to occur. Therefore, to establish whether the Asp172-Asp179 LBHB is the cause of the pH switch observed in BlaC, the mutants D172N and D179N can serve as test cases. ^{1}H-^{15}N TROSY-HSQC spectra were recorded for BlaC D179N and D172N samples at pH values of 5, 6.5, 7, 8, and 9. Interestingly, only a single conformation was evident in the spectra at all pH values, indicating that the pH switch is abolished in these mutants (Figure 3.4c). We conclude that deprotonation of the Asp172-Asp179 pair is the cause of the conformational change and propose that repulsion between the two negatively charged carboxy groups destabilizes the closed form of the Ω-loop, leading to unfolding of the loop and enhancing ceftazidime hydrolysis. In line with this model, the catalytic efficiency of ceftazidime hydrolysis of D179N and D172N mutant does not increase with pH (Table 3.1, Figure S3.2b). Biphasic ceftazidime kinetics with a small amplitude for the first phase are observed for these mutants (Table 3.1), suggesting that a minor state is present at all pH values due to a weaker interaction between residues 172 and 179 causing a slight destabilization of the Ω-loop.[188]

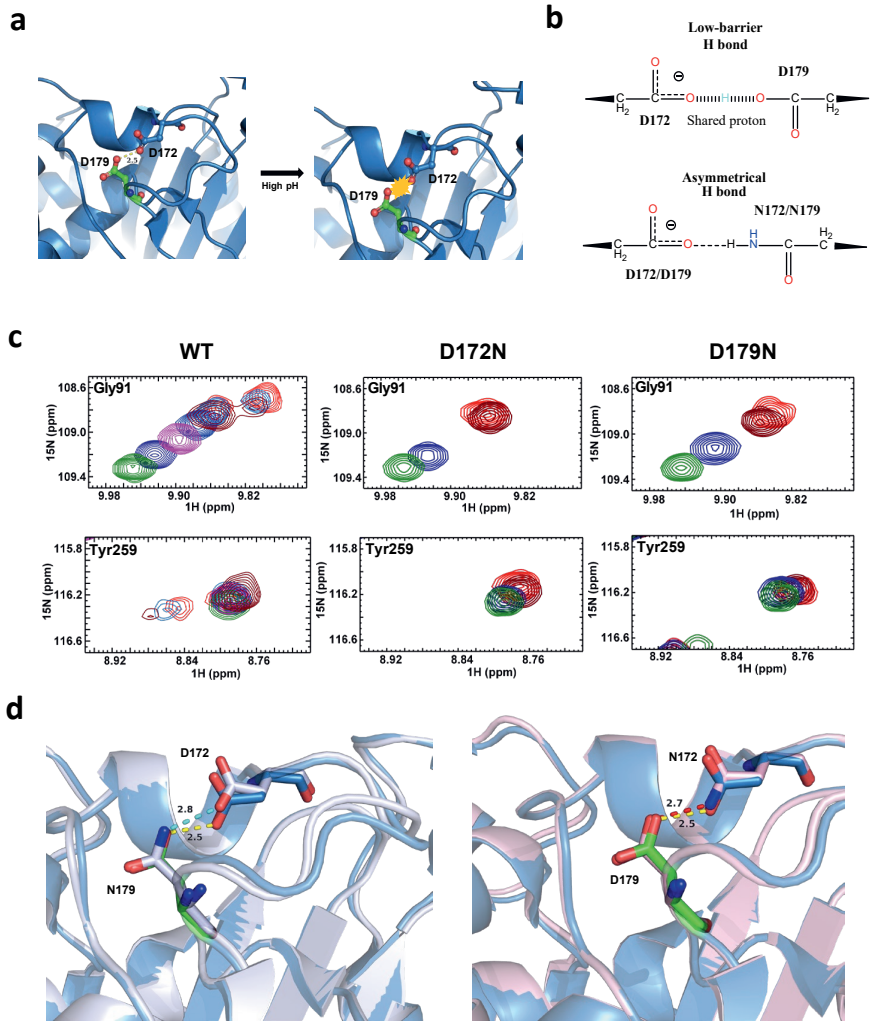

Figure 3.5 The LBHB between Asp179 and Asp172. **a)** The model for Ω-loop destabilization at high pH; **b)** Schematic representation of the hydrogen bonding between residues in positions 172 and 179 in BlaC WT and the D172N/D179N variants; **c)** Details of ^{1}H-^{15}N TROSY HSQC spectra for the amide resonances of residues Gly91 and Tyr259 in WT BlaC, mutant D172N, and mutant D179N at different pH values. The data were collected at 25 °C in 100 mM NaPi buffer; **d)** Conformational changes caused by the D179N (white, left, PDB ID 8BTU[188]) and D172N (pink, right, PDB ID 7A5W[158]) mutations. The potential LBHB in BlaC WT (blue, PDB ID 2GDN[72]) is represented by yellow dashed lines. The potential standard H-bonds in D179N and D172N are shown as cyan and red dashed lines, respectively. Indicated distances are in Å.

Discussion

In the general description of the mechanism of serine β-lactamases, it is well-established that Glu166 has an important role in proton transfers during the catalytic reactions.[65,66,142,193-195] Mutagenesis of this residue lowers the activity towards penicillins and early cephalosporins[181,182,184-186,196] but hydrolysis of ceftazidime appears unaffected.[133,155,197,198] A recent laboratory evolution study also indicated that ceftazidime conversion by CTX-M does not require the conserved Glu166.[133,199] In the case of the TEM-1 mutant W165Y/E166Y/P167G, Tyr166 appeared to take over the role of the Glu, accompanied by a shift in the optimal pH.[14] In the current study, we observed that BlaC E166A is more, not less active against ceftazidime than the WT enzyme, supporting the conclusion that Glu166 is not required for conversion of this substrate. The mechanism of water activation in the absence of the Glu is unclear, but previous studies have indicated that substitutions at Glu166 have the potential to lower the pK_a values of Lys73, making alternative pathways for proton transfer possible.[64,75]

Our study shows that BlaC WT undergoes a structural change at high pH that closely resembles what has been observed for BlaC P167S at neutral pH. For this mutant it was shown that the Ω-loop opens widely in the deprotonated state, displaying an enhanced hydrolysis rate of ceftazidime, whereas the turnover of the closed state is low, due to very slow deacylation. The reaction rate is high in the beginning (first phase), but the interconversion between open and closed states results in removal of the open state and accumulation of the closed state during the reaction (second kinetic phase). When all substrate is converted, the open state reappears.[179] Given the similarity in NMR spectral changes and kinetic profiles, it is highly likely that the same phenomenon underlies the biphasic kinetics observed for BlaC WT at high pH. The structural change mostly affects the Ω-loop and it is known that its restructuring is important for ceftazidime binding, because the loop lines one site of the active site and limits access of bulky substrates. However, it is not obvious which deprotonable group is responsible for the pH dependent shift in structure. The prevalent side chain interactions within the Ω-loop of class A β-lactamases involve Arg161-Asp163, Glu166-Asn170, and Arg164-Asp179.[126,127,129,200] Changes in both Arg164 and

Asp179 disrupt the salt bridge that they form, resulting in an elevation of resistance against ceftazidime, accompanied by a reduction in resistance to other β-lactam antibiotics.[112,113,129,201-204] In KPC-2, mutation of Asp179 also resulted in shifts in the position of Ser70, Glu166, and Asn170.[200] An increase in the flexibility of the Ω-loop was observed in the crystal structure of PC1 D179N from *Staphylococcus aureus*.[127] However, the conserved interaction between Arg164 and Asp179 is absent in BlaC, because position 164 is occupied by Ala rather than Arg. Instead, Asp179 shares a LBHB with Asp172 that can provide stability to the Ω-loop. LBHBs occur between two functional groups with similar pK_a values, equally sharing a proton, which results in the formation of a short (~2.5 Å) hydrogen bond that is 5 to 10 times stronger than that of a typical hydrogen bond.[205,206] Interestingly, another, conserved, LBHB is found in β-lactamases, for Asp233-Asp246, stabilizing two strands of the β-sheet and also relevant for the substrate specificity.[207, 208] To test whether the Asp172-Asp179 LBHB was deprotonated at high pH, the mutants D172 and D179N were studied, both showing no titratable appearance of double peaks in NMR spectra, indicating the absence of a large structural change. The conversion rates of ceftazidime are not strongly pH dependent, but, interestingly, do show slight biphasic behavior, also at neutral pH. We explain this by assuming that the regular H-bonds in the mutants are weaker than the LBHB, leading to a slight destabilization of the Ω-loop at all pH values, in line with an earlier study on the D179N mutant.[188] The pK_a of the deprotonation of Asp172-Asp179 depends on the surrounding structure. In the mutant P167S, the Ω-loop is strongly destabilized, resulting in a pK_a of 6.7, whereas phosphate binding stabilizes the structure, leading to an increase in the pK_a from 8.9 to 9.8 for BlaC WT.

Conclusions

Substrate specificity is considered a key feature of modern enzymes. It depends on multiple precise interactions between enzyme and substrate in the Michaelis complex and the transition state. Such interactions need to be optimized by evolution to achieve high turnover rates. At the same time, enzymes must evolve to adapt under

changing selection pressures. The research on β-lactamases shows that it is relatively easy to change substrate preferences. Residues such as Glu166 and Asn170 located in the Ω-loop are part of the active site and need to be positioned precisely for optimal catalysis. The loop is, however, easily destabilized and restructured by mutations, or even a pH change, as shown in the current work, creating a much wider active site pocket that allows for larger β-lactam compounds to bind. Such restructuring may displace catalytic residues, for example Glu166 in the BlaC P167S variant. In the case of ceftazidime, however, catalysis at a low turnover rate takes place without Glu166. Such a variant may serve as the starting point of further optimization by evolution under conditions in which ceftazidime represents the selection pressure. Laboratory evolution experiments can be used to determine how such optimization would change the enzyme and are ongoing.

Materials and Methods

Antimicrobial susceptibility testing

Antibiotic resistance was tested in the *E. coli* cells carrying pUK21-*blaC* plasmids with the gene behind the *lac* promotor. Drops of 10 µL of *E. coli* cultures with optical densities (OD_{600}) of 0.3, 0.03, 0.003 and 0.0003 were applied on the LB plates containing 50 µg mL^{-1} kanamycin and 1 mM IPTG, and various concentrations of ceftazidime or ceftriaxone. The plates were incubated at 23 °C, 30 °C or 37 °C until growth was visible.

Protein production and purification

The genes for BlaC WT, E166A, D179N and D172N were cloned into pET28a plasmids downstream of an N-terminal His-tag and a TEV cleavage site (Figure S3.5) and expressed in *E. coli* BL21 (DE3).[179] The proteins were produced and purified according to previously described protocols.[149] Pure protein was stored at -80 °C in 50 mM Tris and 50 mM NaCl (pH 7).

Enzyme kinetics

In vitro kinetic parameters were determined by monitoring the absorption change at 486 nm for nitrocefin ($\Delta\varepsilon_{486}$ = 11300 $M^{-1}cm^{-1}$)[159] with a TECAN infinite® M1000PRO plate reader. The extinction coefficients for ceftazidime ($\Delta\varepsilon_{260}$ = 7 ± 1 $mM^{-1}cm^{-1}$), cefepime ($\Delta\varepsilon_{260}$ = 10.4 ± 0.8 $mM^{-1}cm^{-1}$), cefoxitin ($\Delta\varepsilon_{260}$ = 8.3 ± 0.4 $mM^{-1}cm^{-1}$), cefuroxime ($\Delta\varepsilon_{260}$ = 8.3 ± 0.5 $mM^{-1}cm^{-1}$), ceftriaxone ($\Delta\varepsilon_{260}$ = 7.8 ± 0.4 $mM^{-1}cm^{-1}$) were determined using a thermostatic PerkinElmer Lambda 1050+ UV-Vis spectrometer. For ampicillin and meropenem $\Delta\varepsilon_{235}$ = 861 $M^{-1}cm^{-1}$ [158] and $\Delta\varepsilon_{297}$ = 7.3 $mM^{-1}cm^{-1}$ (M. Radojkovic, personal communication) were used, respectively. All kinetic measurements were performed in triplicate in 100 mM NaPi buffer (pH 5, 6.5, 7, 8, 8.5 or 9) at 25 °C. For nitrocefin kinetics 20 nM BlaC WT or 70 nM E166A mutant was used, and the reaction was followed for 5 min. The initial velocities were fitted to the Michaelis-Menten equation:

$$v_{\mathrm{i}} = \frac{k_{\mathrm{cat}}[E][S]}{K_{\mathrm{M}}+[S]} \tag{3.1}$$

Where v_i is the initial velocity, k_{cat} is the turnover number and K_{M} is the apparent Michaelis constant. The hydrolysis reaction comprises several steps, so the definition of this constant differs from the standard one and is thus considered an apparent K_{M}.[179] [E] and [S] are the enzyme and substrate concentrations, respectively. To measure the ceftazidime and cefepime hydrolysis at various concentrations and pH values, 1 µM BlaC WT, 1 µM BlaC E166A, 0.5 µM BlaC D172N or 0.5 µM BlaC D179N were used. Reactions were followed for 5 min and performed in triplicate. For ceftazidime or cefepime hydrolysis, determination of k_{cat} was not possible due to the high $K_{\mathrm{M}}^{\mathrm{app}}$, therefore equation 3.2 was used, as the limiting case of equation 1 ([S] << K_{M}), to determine the catalytic efficiency ($k_{\mathrm{cat}}/K_{\mathrm{M}}$):

$$v_{\mathrm{i}} = \frac{k_{\mathrm{cat}}}{K_{\mathrm{M}}}[E][S] \tag{3.2}$$

NMR spectroscopy

Backbone assignments for 0.5 mM [^{15}N, ^{13}C] BlaC WT were obtained with standard HNCA and TROSY-HSQC experiments that were recorded on a Bruker AVIII HD 850 MHz spectrometer with a TCI cryoprobe at 25 °C in 100 mM NaPi buffer at pH 8, with 1 mM TSP (trimethylsilylpropanoic acid) and 6% D_2O. Data were processed with Topspin 4.1.1 (Bruker Biospin) and analyzed using CcpNmr version 2.[161] The spectrum was assigned with the HNCA and the WT spectra at pH 6.5 (BMRB ID: 27067).[149] TROSY-HSQC and HNCA spectra of BlaC E166A were obtained in 100 mM NaPi buffer at pH 6.5 at 25 °C. The assignments for BlaC WT at pH 8 and BlaC E166A at pH 6.4 have been deposited in the BMRB under access codes 52198 and 52201, respectively. The average chemical shift differences $\Delta\delta$ between the two states observed for BlaC of the ^{1}H ($\Delta\delta_1$) and ^{15}N ($\Delta\delta_2$) resonances of backbone amides were calculated with equation 3.3.

$$\Delta\delta = \sqrt{\frac{1}{2}\left[{\Delta\delta_1}^2 + \left(\frac{\Delta\delta_2}{5}\right)^2\right]} \tag{3.3}$$

For the pH titration, samples were prepared in 100 mM NaPi, MES, Tris, or HEPES (with the addition of 6% D_2O and 1 mM trimethylsilylpropanoic acid) in the pH range

5-10. Titrations of BlaC WT with NaPi were performed at pH 8. As the phosphate concentration increased from 10 mM to 250 mM, the protein concentration decreased from 150 to 113 μM.

Protein crystallization

Crystallization conditions for BlaC E166A and BlaC WT at a concentration of 10 mg mL^{-1} were screened by the sitting-drop method using the JCSG$^+$, BSC, PACT, and Morpheus (Molecular Dimensions, Catcliffe, UK) screens at 20 °C with 200 nL drops with a 1:1 protein to screening condition ratio.[163] Crystals for BlaC E166A grew within two weeks in 0.05 M $LiSO_4$, 0.1 M sodium acetate buffer, pH 4.5, with 25% w/v polyethylene glycol (PEG) 8000 as precipitant or 0.1 M MB1 buffer (1 M imidazole and 1 M MES monohydrate) pH 6.5, 0.06 M halogens, with 44.29% w/v M1K3350 (12% w/v PEG 1000, 12% w/v PEG 3350, and 12% v/v MPD; original solution Molecular Dimensions) as precipitant. The crystals for BlaC WT grew within two weeks in 0.1 M Tris buffer, pH 8, with 20% w/v PEG 6K as precipitant and 0.01 M $ZnCl_2$ as salt. After one month the crystals were mounted on cryoloops in mother liquor, with the addition of 25% glycerol and flash frozen in liquid nitrogen for X-ray data collection.

Data collection, processing, and structure refinement

Diffraction data for the BlaC WT at pH 8 and BlaC E166A mutant at pH 4.5 and 6.5 structures were collected at the European Synchrotron Radiation Facility on the MASSIF beamline.[164] The resolution cutoff was determined based on completeness and CC1/2 values. The data were indexed and integrated using DIALS[164] and scaled using Aimless.[166] The structures were solved by molecular replacement using MOLREP from the CCP4 suite[167] by the PDB entry 2GDN[72] as the model for molecular replacement. Model building and refinement were performed in Coot and REFMAC.[209] Waters were added in REFMAC during refinement. The models were further optimized using the PDB-REDO web server.[168] The refinement and data collection statistics are given in the supplementary information (Table S3.2). The structures of E166A at two pH values and the BlaC WT have been deposited in the Protein Data Bank.

Supporting information

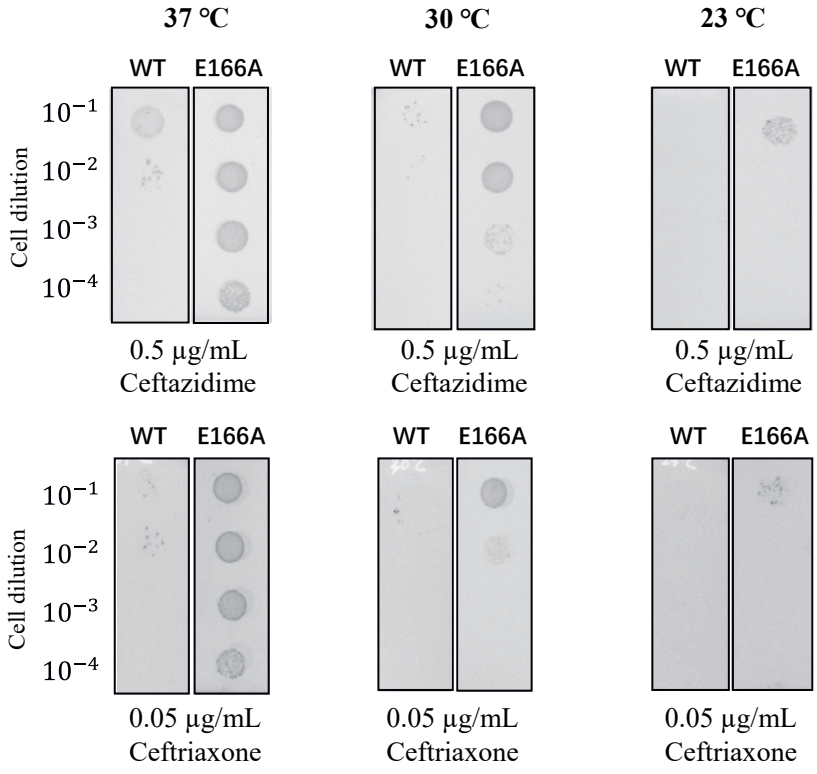

Figure S3.1 The activity of BlaC WT and BlaC E166A in *E. coli* on LB-agar plates. Cells were spotted in increasing dilution on plates that contained either 0.5 µg mL^{-1} ceftazidime or 0.05 µg mL^{-1} ceftriaxone as well as kanamycin (50 µg/mL) to ensure plasmid stability and 1 mM IPTG to induce gene expression. The *blaC* gene with a TAT signal peptide for translocation to the periplasmic space was inserted behind the *lac* promotor in pUK18.[210] The plates were incubated at 37 °C for 14 h, 30 °C for 18 h, and 23 °C for 2 days

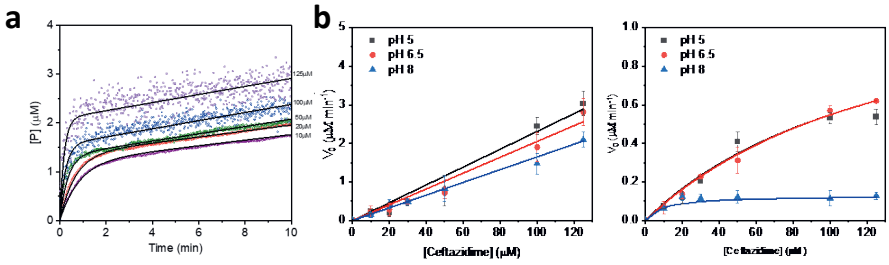

Figure S3.2 Ceftazidime hydrolysis kinetics. **a)** Biphasic kinetics of ceftazidime hydrolysis. Product curves of ceftazidime hydrolysis by BlaC WT at pH 8 in phosphate buffer at various substrate concentrations (10, 20, 50, 100, and 125 μM). The black line is the fit for the equation for biphasic kinetics;[179] **b)** Ceftazidime kinetics by BlaC D179N at pH 5, 6.5, and 8 in phosphate buffer. The left and right graphs show the data for the first and second phase of the reaction, respectively. Error bars represent the standard deviation of triplicate measurements.

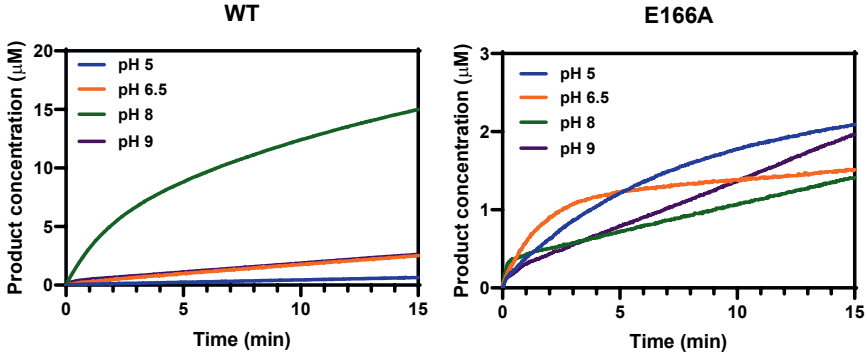

Figure S3.3 Cefepime hydrolysis at 25 ˚C at different pH values. The initial concentrations of cefepime and BlaC were 25 μM and 1 μM, respectively.

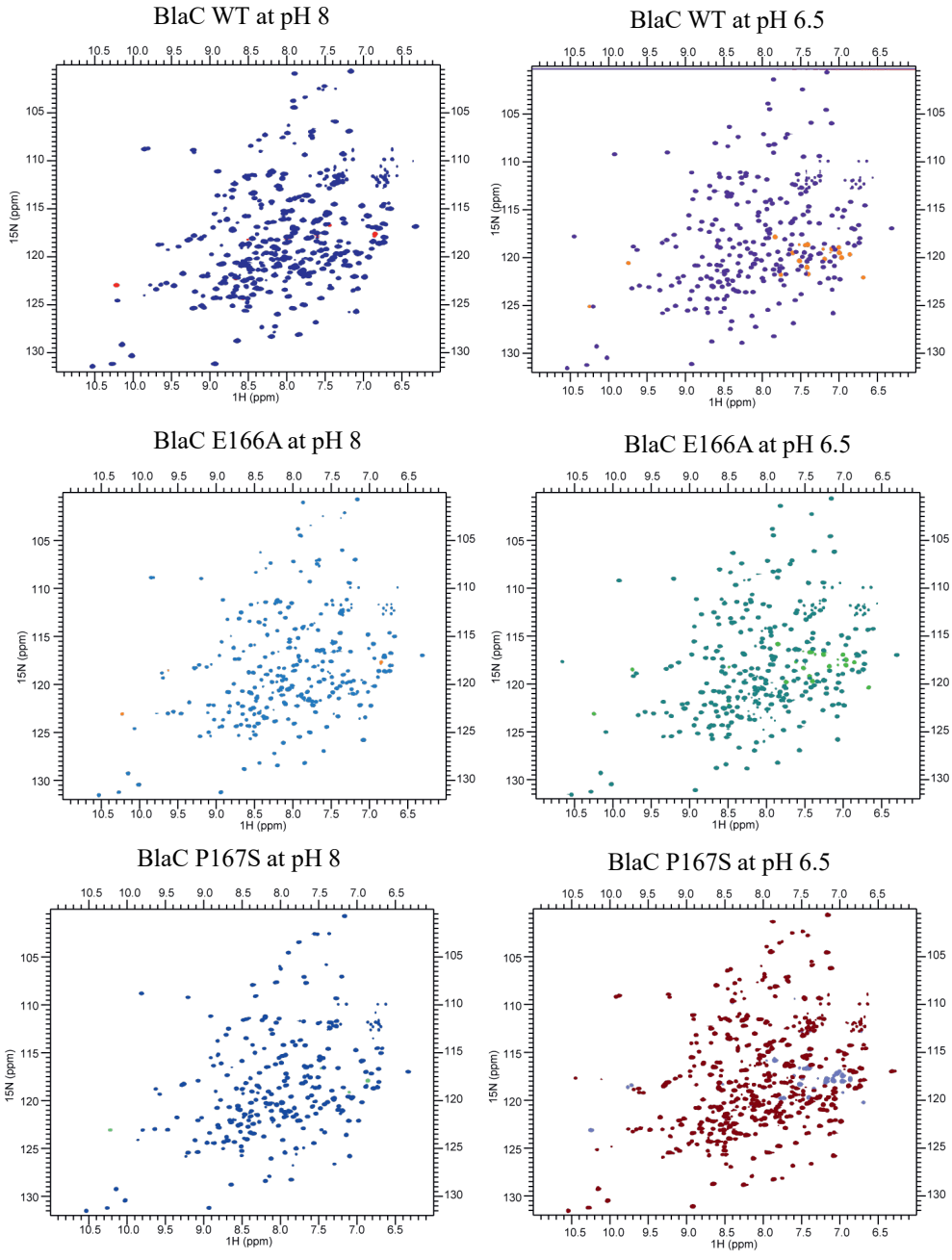

Figure S3.4 TROSY-HSQC spectra of BlaC WT and mutants at pH 6.5 and 8 in 100 mM NaPi buffer at 25°C. Peaks in the less abundant colors are folded into the spectrum.

```
                                  30         40         50         60
MGSSHHHHHH SSGLVPRGSH MENLYFQGDL ADRFAELERR YDARLGVYVP ATGTTAAIEY

        70         80        90         101        111        121
RADERFAFCS TFKAPLVAAV LHQNPLTHLD KLITYTSDDI RSISPVAQQH VQTGMTIGQL

       132        142        148        158        168        178
CDAAIRYSDG TAANLLLADL GGPGGGTAAF TGYLRSLGDT VSRLDAEEPE LNRDPPGDER

       188        198        208        218        228        238
DTTTPHAIAL VLQQLVLGNA LPPDKRALLT DWMARNTTGA KRIRAGFPAD WKVIDKTGTG

       249        260        270        280        290
DYGRANDIAV VWSPTGVPYV VAVMSDRAGG GYDAEPREAL LAEAATCVAG VLA
```

Figure S3.5 The amino acid sequence of BlaC WT used for *in vitro* experiments. Residues of the TEV-cleavable His-tag are highlighted in grey. Residues 28-293 correspond to residue numbers 43-307 of the BlaC Uniprot sequence P9WKD3-1 and are numbered according to the Ambler notation.

Table S3.1 Data collection and refinement statistics for the structures of BlaC E166A and WT.

Data collection	E166A pH 4.5	E166A pH 6.5	WT pH 8
Wavelength (Å)	0.87Å	0.98Å	0.87Å
Resolution (Å)	54.74 (1.44) 1.42-1.44	40.01 (2.3) 2.3-2.38	38.45 (1.84) 1.8-1.84
Space group	P1 21 1	P21 21 21	P21 21 21
Unit cell a, b, c (Å)	38.95 54.74 53.75	53.85 54.68 80.01	54.13 54.63 80.14
Unit angle α, ß, γ	90.0 92.8 90.0	90.0 90.0 90.0	90.0 90.0 90.0
CC1/2	85.3 (57.5)	87.9 (76.3)	99.5 (58.8)
Rpim (%)	16.1 (64.4)	24.8 (41.4)	6.5 (45.9)
|I/σI|	8.0 (1.1)	4.5 (2.2)	9.7 (1.7)
Completeness (%)	99.3 (96)	99.8 (99.9)	97.6 (71.7)
Multiplicity	1.9	1.9	1.9
Unique reflections	42646	20049	22101
Refinement			
Atoms protein/ligands/water	1985/22/201	1985/0/78	1988/18/137
B-factors protein/ligands/water ($Å^2$)	17/39/31	29/0/28	19/34/29
Rwork/R free (%)	17.3/22.0	27.5/32.3	16.0/21.2
Bond lengths RMSZ/RMSD (Å)	0.76/0.013	0.25/0.010	0.44/0.015
Bond angles RMSZ/RMSD (Å)	0.84/1.75	0.49/1.44	0.65/2.09
Ramachandran plot preferred/outliers	252/2	245/2	253/2
Ramachandran plot Z-score	-0.258	-2.7	0.228
Clash score	4.78	9.6	5.02
MolProbity score	1.28	2.2	1.4